Supporting Information

3D Printed Microstructured Ultra-Sensitive Pressure Sensors Based on Microgel-Reinforced Double Network Hydrogels for Biomechanical Applications

Jingxia Zheng†[a], Guoqi Chen†[a], Hailong Yang[a], Canjie Zhu[a], Shengnan Li[a], Wenquan Wang[b], Jiayuan Ren[a], Yang Cong[a], Xun Xu[c], Xinwei Wang[c], Jun Fu[a]*

Experimental Section

Materials. 2-acrylamido-2-methyl propane sulfonic acid (AMPS, 98%), acryloxyethyltrimethyl ammonium chloride (DAC, 99%), acrylamide(AAm, 99%), acrylic acid (AAc, 99%), 2-hydroxy-4'-(2-hydroxyethoxy)-2-methylpropiophenone (I2959, 98%), N, N, N', N'-tetramethylethylenediamine (TEMED, 99%) were purchased from Aladdin (Shanghai, China); N, N'-methylenebisacrylamide (MBAA, 99%), Cyclohexane (99.5%), Span80 (pharmaceutical grade) were acquired from Macklin (Shanghai, China); ethanol (99.7%) was purchased from Greagent (Shanghai, China). All these reagents are used as received. Deionized water was prepared in laboratory.

Preparation of microgels. We dissolve 30 wt% AMPS, 4 mol/% MBAA, 4 mol/% I2959 (relative monomer content), 10μL TEMED in deionized water to form the disperse phase, which was ultrasonic vibration emulsified with cyclohexane containing 3 wt% Span80 to obtain the water/oil (W/O) emulsion. Then, the W/O emulsion was irradiated at UV light for 20 min to form microgels. To purify the microgels, the PAMPS microgels were transferred to ethanol and centrifuged at 4000 rpm for 10 min, then discarded the supernatant, and the process was repeated thrice with ethanol and

thrice with water. Finally, the PAMPS microgels were freeze-dried to obtain dry fine powders. The PDAC and PAAm microgels are prepared in the same way.

Preparation of Jammed microgel inks. Jammed microgel ink is obtained by adding 5 wt% PAMPS microgel fine powders into an aqueous solution of acrylic acid (AAc), N, N'-methylenebisacrylamide (MBAA) and 2-hydroxy-4'-(2-hydroxyethoxy)-2-methylpropiophenone (I2959) to absorb the solution overnight to achieve adequate swelling.

Preparation of DN hydrogels. The microgel precursor with different formulations were quickly transferred into a template. Free radical polymerization was initiated and took place at 25 °C for 15 min by UV light to obtain microgel-reinforced double network (MRDN) hydrogels.

3D printing. The target shapes were designed in 3D Bulider or 3Ds Max and exported as STL files, then printed them by using a 3D bioprinter (Regenovo 3D Bio-Architect ℝ Sparrow). The jammed microgel ink was transferred into a 5ml syringe, and all structures were extruded and printed by a 210um diameter needle, using the same print settings: a layer height 300 μm, line width 300 μm, a print speed 8-10 mm s^{-1} and a pressure applied to the piston of 0.2-0.3 MPa. All printed structures were printed on the PE film substrate of 0.1mm. After printing, the constructs are exposed to UV light to initiate free radical polymerization of AAc monomer to form a second network interpenetrating throughout the microgels.

Rheology measurements. Rheology measurements were carried out by using a rotational rheometer (Anton-Paar MCR302, Austria) with a parallel plate (25 mm

diameter rotating top plate) at 25 °C. The viscosity of jammed microgel inks were measured by shear rate sweeps in a range from 0.01-100 s^{-1}. The amplitude sweep was carried out on jammed microgel inks at 1 Hz in a strain range from 0.1-1000%. The dynamic strain step tests were carried out by using 100% and 1% strain for 60 s, respectively for three cycles, and each sweep interval was 10s. The creep resistance tests of jammed microgel inks were analyzed by transient test: the samples were loaded under 1 Pa stress for 180s, and then maintained for 60s to monitor the creep recovery behavior of them.

Mechanical Characterization: Tensile, compression and cyclic loading–unloading tests of the MRDN hydrogel were carried out using a Universal Testing Machine (CMT1104, Zhuhai SUST Electronic Equipment CO., China) equipped with a 200 N and a 10000 N load cell at 25 °C.

The dumbbell-shaped samples (35 mm × 2.0 mm × 1.5 mm, gauge length for 20 mm) for tensile tests were stretched at a constant velocity of 50 mm min^{-1}. Engineering tensile stress–strain curves were recorded. The fracture stress σ_b and fracture strain ε_b were the values at fracture point. The Young's modulus was determined from the slope within the initial linear region (less than 10% strain) of the stress-strain curve. The toughness was calculated as the area below the stress-strain curve of a sample until fracture. At least three specimens were tested for each sample. And the average values and standard deviations were reported.

Compressive tests were carried out on cylindrical samples with a diameter of 10 mm and height of 5 mm at 0.5 mm/min up to 85 % strain. The compressive strength σ_c was

the values at the point of 85% strain. For cyclic compression loading–unloading tests, the samples were repeatedly loaded to 85 % strain and unloaded at 0.5 mm min^{-1}. At least three specimens were tested for each sample, and one specimen was selected for reporting.

Micromorphology Characterization: Rhodamine B was added to the jammed microgel inks to allow them to be observed the size under the optical microscope. The MRDN hydrogel was immersed in 3 vol/% acetic acid solution containing 0.5 wt/% Alixin blue dying for 15min, and then rinsed it with deionized water. We observed the morphological changes of the MRDN hydrogels before and after stretching with optical microscope.

The grain size distribution of the PAMPS microgels was measured using a laser particle analyzer (Topsizer, China).

Conductivity Characterization: The ionic conductivity (σ) of DN hydrogels was calculated from the surface area (S) and thickness (d) of themselves and the resistance (R) measured by the electrochemical AC impedance method of the electrochemical workstation (CHI660E, China), which was defined as $\sigma = \dfrac{d}{RS}$. At least three specimens were tested for each sample. And the average values and standard deviations were reported.

Connect the hydrogel to the power supply (3V) and an LED bulb, and observe the light emission of the bulb.

Sensing Characterization and Human Monitoring: The sensing tests are carried out by resistance-capacitance tester (01RC, Linkzill, China). Connect both ends of the

dumbbell-shaped DN hydrogels with copper wires to obtain strain sensors, apply tension to it to test its GF, response time and cyclic tensile sensing, etc. The GF defined as $GF=|\Delta R/R_0|/\varepsilon$, where ε is the strain, $\Delta R/R_0=|R-R_0|/R_0$, with R_0 as the initial resistance and R for that under strain.

Connect copper wires on the two surfaces of cylindrical or 3D printing pyramid, hemisphere, cube-shaped MRDN hydrogels to obtain pressure sensors, and apply pressure to test its sensitivity, response time and cyclic compressive sensing. The sensitivity(S) is defined as $|\Delta R/R_0|/p$, where p is the pressure, $\Delta R/R_0=|R-R_0|/R_0$, with R_0 as the initial resistance and R for that under strain.

Attach the dumbbell-shaped hydrogel strain sensor to human fingers, wrists, elbows, knees, laryngeal nodules and soles for human monitoring such as fingers, wrists, elbows and knees bending, swallowing, walking and running.

Assemble a wearable shoe-pad based on the eight-channel pressure sensors for human gait monitoring. The volunteer signed an informed consent before performing this experiment.

Construct a flexible sensor array with pyramid, hemisphere and cube microstructures on the surface, and place a small tortoise (about 5 g weight) on the microstructured sensor array and track its trajectory as it crawls across the array of pyramids, hemispheres, and cubes, then record the signal change of the resistance change rate during the crawling process. The animal tests are performed with ethical approval from the Institutional Animal Care and Use Committee of Sun Yat-sen University (Approval No. SYSU-IACUC-2023-B0115). All experiments were

performed in compliance with the SYSU's policy on animal use and ethics.

Finite element analysis (FEA): The stress distribution of hydrogels with different microstructures under external stress was investigated by using Abaqus CAE software for finite element analysis. The modeling of microstructure models is carried out in Solidworks software.

Table S1. Formulations and nomenclatures of MRDN hydrogels

Sample	Mic-PAMPS (wt/%)	AAc (wt/%)	MBAA (mol/%)	I2959 (mol/%)
Mic-PAMPS$_1$/PAAc$_{30}$	1	30	0.05	0.05
Mic-PAMPS$_2$/PAAc$_{30}$	2	30	0.05	0.05
Mic-PAMPS$_3$/PAAc$_{30}$	3	30	0.05	0.05
Mic-PAMPS$_4$/PAAc$_{30}$	4	30	0.05	0.05
Mic-PAMPS$_5$/PAAc$_{30}$	5	30	0.05	0.05
Mic-PAMPS$_3$/PAAc$_{10}$	3	10	0.05	0.05
Mic-PAMPS$_3$/PAAc$_{20}$	3	20	0.05	0.05
Mic-PAMPS$_3$/PAAc$_{40}$	3	40	0.05	0.05

Table S2. Young's modulus and sensitivity of different hydrogel-based sensors

Materials	Young's modulus (kPa)	Sensitivity (kPa^{-1})	Ref.
ACC/PAAc/SA	6.7	0.17	1
PAM/PVA/KCl	100	0.05	2
PVA/PAAc-Fe^{3+}	25	0.018	3

|			
GelMA	15	0.19	4
DOPA-PSBMA	1.5	0.096	5
MXene/PHMP	30	0.63	6
PAM/SPNs	255	0.013	7
PMAA-co-DMAPS	130	0.6	8
PNDU-CNF@CNT$_x$	23	1.11	9
PAA-LM/rGO	100	0.85	10
SA/NaCl/PAM	50	1.45	11
Mic-PAMPS/PAAc	155	0.925	**This work**
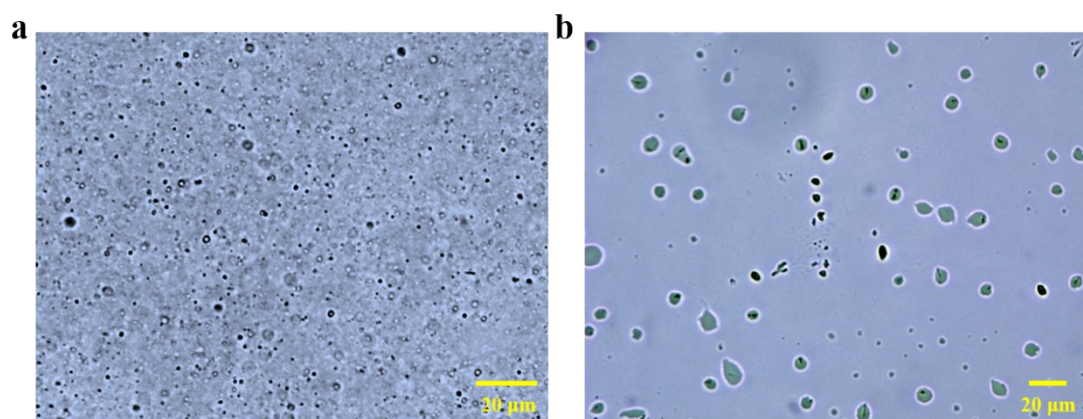
Fig. S1. Optical micrographs of (a) PAMPS microgel emulsion and (b) mic-

PAMPS/PAAc precursor.
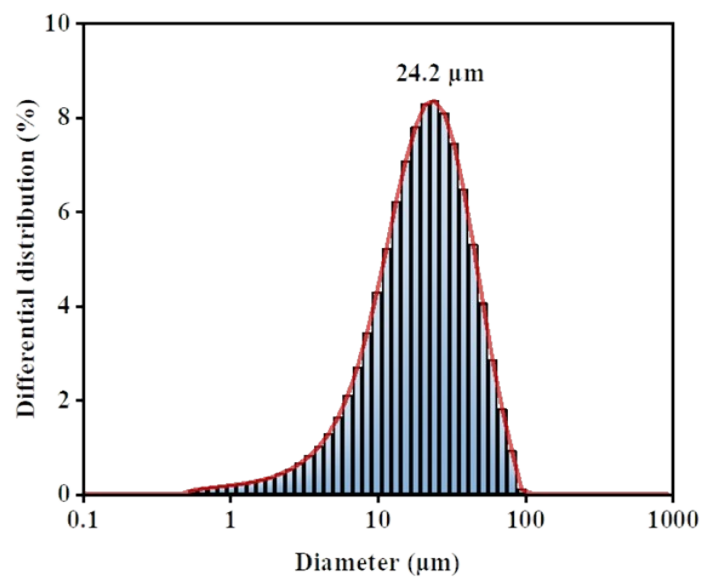
Fig. S2. The differential distribution of diameter of PAMPS microgels.
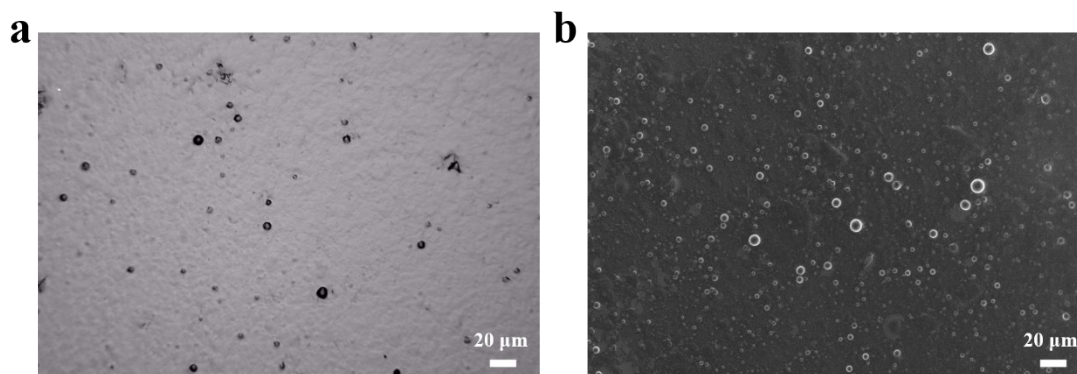
Fig. S3. (a) Optical image and (b) SEM image of freeze-dried gel particles
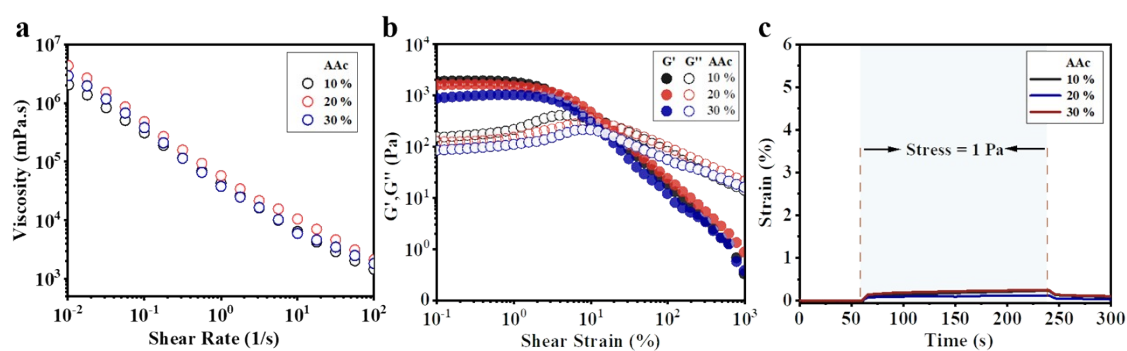
Fig. S4. Rheological properties of the hydrogel precursors with different acrylic acid concentrations at a certain PAMPS microgel concentration. (a) Viscosity-frequency; (b) modulus-strain scans; (c) Representative creep and recovery curves under 1 Pa load.
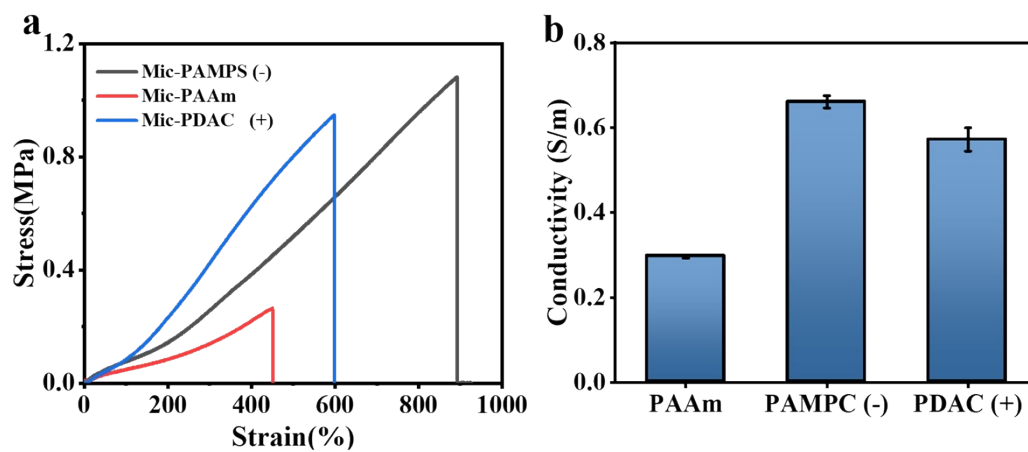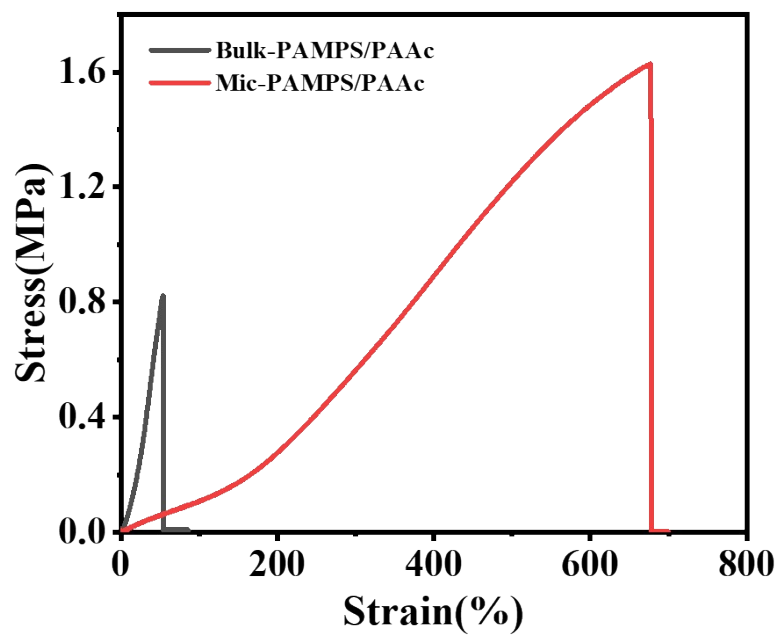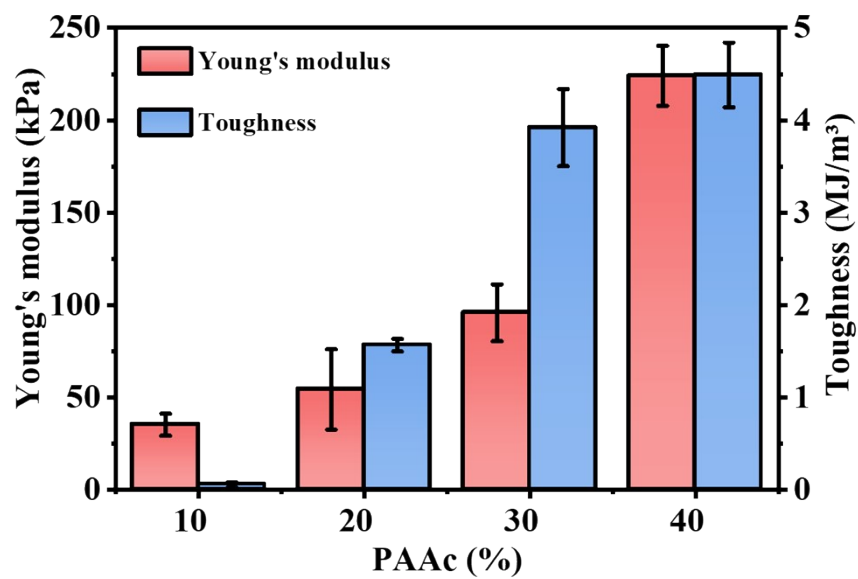
Fig. S5. (a) Mechanical properties and (b) Conductivity of microgels with negative，positive charges or without net charges
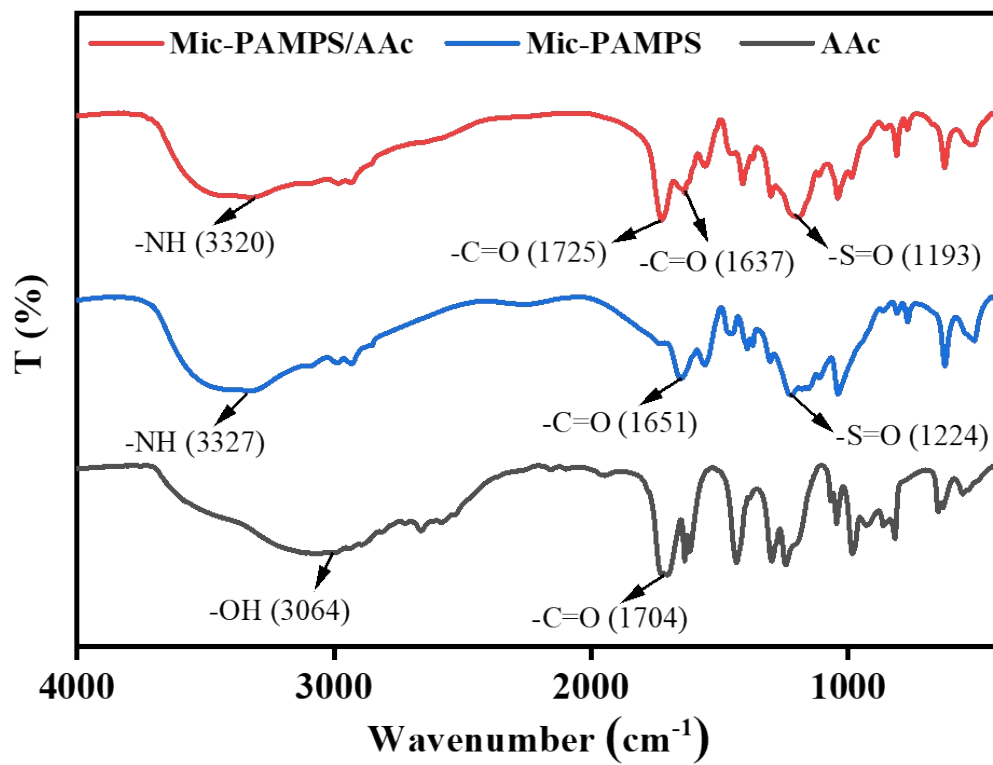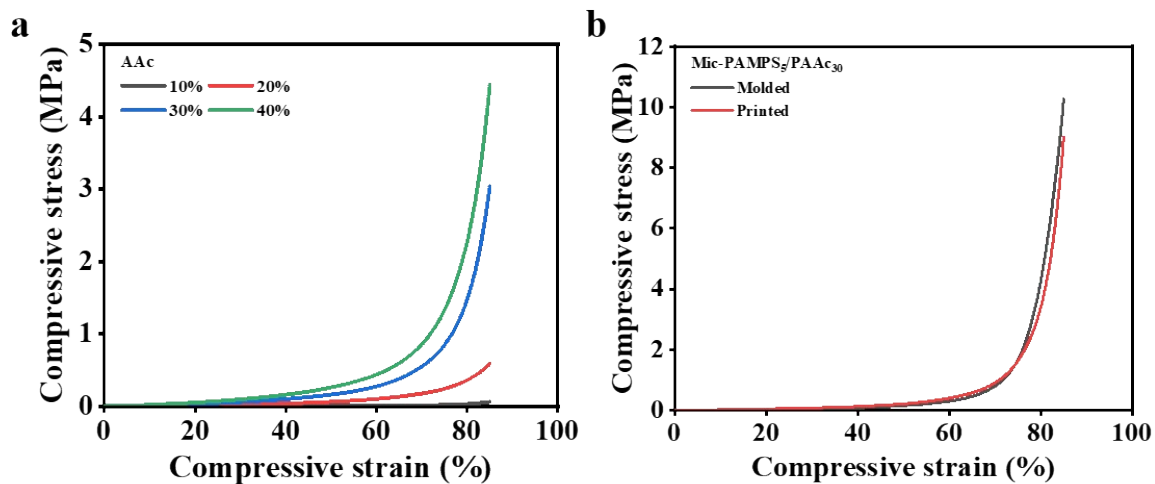
**Fig. S6.** The corresponding FTIR spectra of Mic-PAMPS/AAc, Mic-PAMPS and AAc.

**Fig. S7.** Representative tensile stress-strain curves of the bulk-PAMPS/PAAc gel and the MRDN hydrogel

Fig. S8. Young's modulus and toughness of MRDN hydrogels with 5wt% PAMPS microgels and varying AAc concentrations.
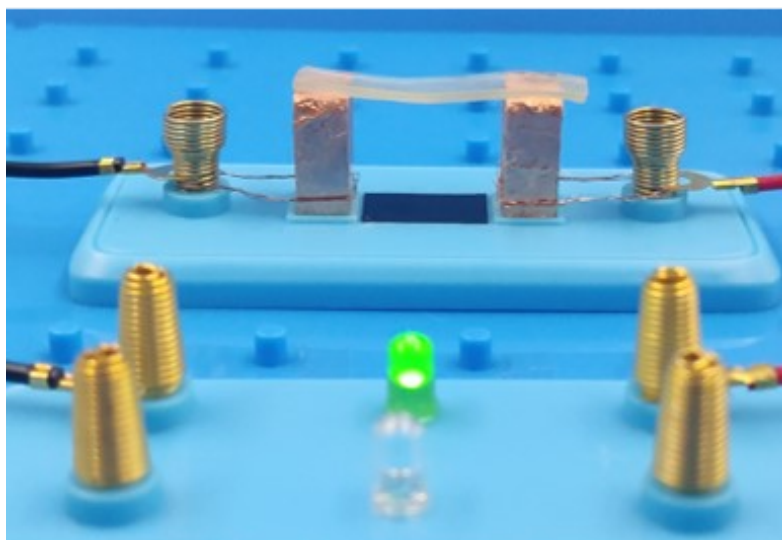
Fig. S9. Representative compressive stress-strain curves of MRDN hydrogels (a) with different AAc concentrations; (b) prepared by injection molding or printing;
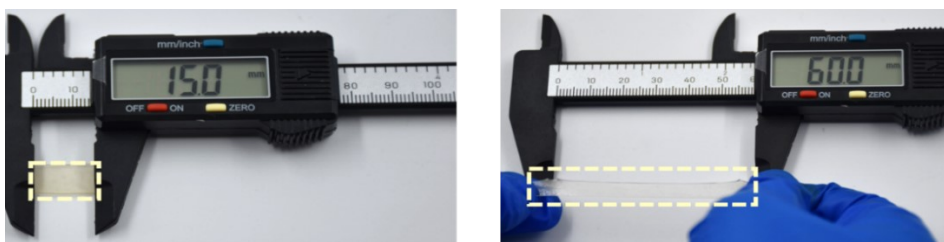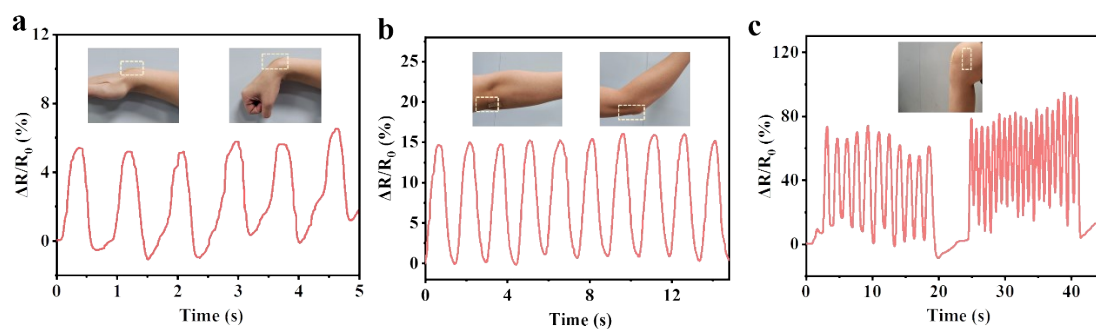
Fig. S10. A printed rectangular hydrogel sample (15mm×5mm×1.5mm) that has been stretched to 400% strain.
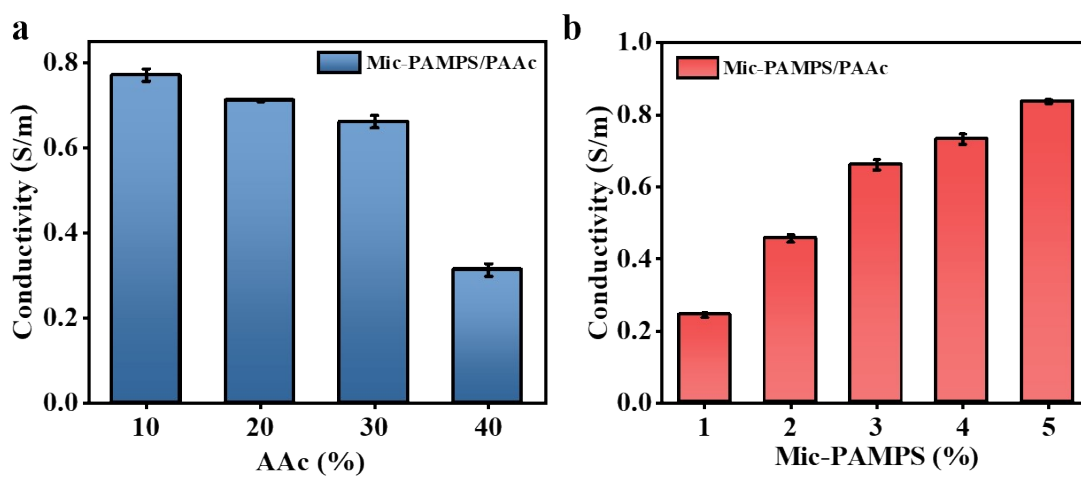

Fig. S11. The ionic conductivity (σ) of MRDN hydrogels fabricated with varying formulations.

Fig. S12. Photograph of MRDN hydrogel fabricated with 5wt% PAMPS microgels

and 30wt% AAc monomers acts as a conductor to make the bulb glow

Fig. S13. The resistance change ratio of the MRDNHs attaching to human (a) wrists,

(b) elbows and (c) knees for monitoring the bending of wrists, elbows and knees.
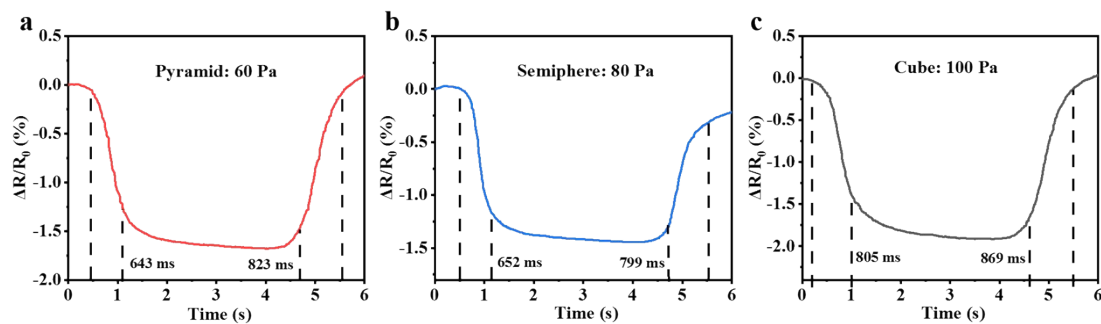
Fig. S14. The pressure limit of detection of (a) the pyramid; (b) the hemisphere; (c) the cube microstructured sensors.

Reference

1   Z. Lei, Q. Wang, S. Sun, W. Zhu and P. Wu, *Adv. Mater.* **2017**, 29, 1700321.

2   G. Ge, Y. Zhang, J. Shao, W. Wang, W. Si, W. Huang and X. Dong, *Adv. Funct. Mater.* **2018**, 28, 1802576.

3   S.-H. Shin, W. Lee, S.-M. Kim, M. Lee, J. M. Koo, S. Y. Hwang, D. X. Oh and J. Park, *Chem. Eng. J.* **2019**, 371, 452-460.

4   Z. Li, S. Zhang, Y. Chen, H. Ling, L. Zhao, G. Luo, X. Wang, M. C. Hartel, H. Liu, Y. Xue, R. Haghniaz, K. Lee, W. Sun, H. Kim, J. Lee, Y. Zhao, Y. Zhao, S. Emaminejad, S. Ahadian, N. Ashammakhi, M. R. Dokmeci, Z. Jiang and A. Khademhosseini, *Adv. Funct. Mater.* **2020**, 30, 2003601.

5   C. Zhang, Y. Zhou, H. Han, H. Zheng, W. Xu and Z. Wang, *ACS Nano* **2021**, 15, 1785-1794.

6   S. He, B. Guo, X. Sun, M. Shi, H. Zhang, F. Yao, H. Sun and J. Li, *ACS Appl. Mater. Interfaces* **2022**, 14, 45869-45879

7   Z. Huang, X. Chen, S. J. K. O'Neill, G. Wu, D. J. Whitaker, J. Li, J. A. McCune and O. A. Scherman, *Nat, Mater,* **2022**, 21, 103-109.

8   Z. Lei and P. Wu, *ACS Nano* **2018**, 12, 12860-12868.

9   L. Jia, S. Wu, R. Yuan, T. Xiang and S. Zhou, *ACS Appl, Mater, Interfaces* **2022**, 14, 27371-27382.

10 Z. Zhang, L. Tang, C. Chen, H. Yu, H. Bai, L. Wang, M. Qin, Y. Feng and W. Feng, *J. Mater. Chem. A* **2021**, 9, 875-883.

11 X. Zhang, N. Sheng, L. Wang, Y. Tan, C. Liu, Y. Xia, Z. Nie and K. Sui, *Mater. Horiz.* **2019**, 6, 326-333.